Supporting Information

Berriman et al. 10.1073/pnas.0902977106

SI Text

Tomographic Volume Analysis. Segmentation of tomographic volumes was performed by drawing contours manually on sections with the segmentation editor and edge detection facility of Amira (Visage Imaging). The path of the VWF tubules within the WPB was determined by a search of the helical model of the tubule against the masked WPB using a 2D template matching technique. The central slice of the helical model was cross-correlated against each slice of the masked WPB for in plane rotations in the range [−60°, 60°] with a step of 0.2°, using a normalized cross-correlation function from Matlab with Image Processing Toolbox (MathWorks). The correlation peaks were manually connected using Amira yielding a three dimensional trace of each tubule. The tubule trace was re-sampled using 3D piecewise cubic Hermite interpolation (Matlab) to obtain a regularly dense sampling and smooth path for further calculations. For each point of each tubule, the minimum inter-tubule distance and minimum tubule-to-membrane mask distance was calculated using a Matlab script.

Ribosome-Sized Densities. Ribosome-sized densities were identified in the tomogram in Movie S2 using a template matching technique. Fifty-four unique projections of an 80S ribosome model, emd1093 (1), were cross-correlated against 20 projected sections (±10 in Z) for each Z section of the tomogram using a normalized cross-correlation function from Matlab with Image Processing Toolbox (Mathworks). The correlation peaks were thresholded using Amira (Visage Imaging). Peaks were clustered and centroids determined. Projected density for each candidate ribosome was calculated using 20 Z sections centered on the centroid. The projections that did not contain particles (without a regard for size) were manually removed, resulting in 380 candidate ribosome positions. The sum of these projections was compared with the sum of 100 equiangular projections of the search model.

1. Spahn CM, et al. (2004) Cryo-EM visualization of a viral internal ribosome entry site bound to human ribosomes: the IRES functions as an RNA-based translation factor. *Cell* 118:465–475.

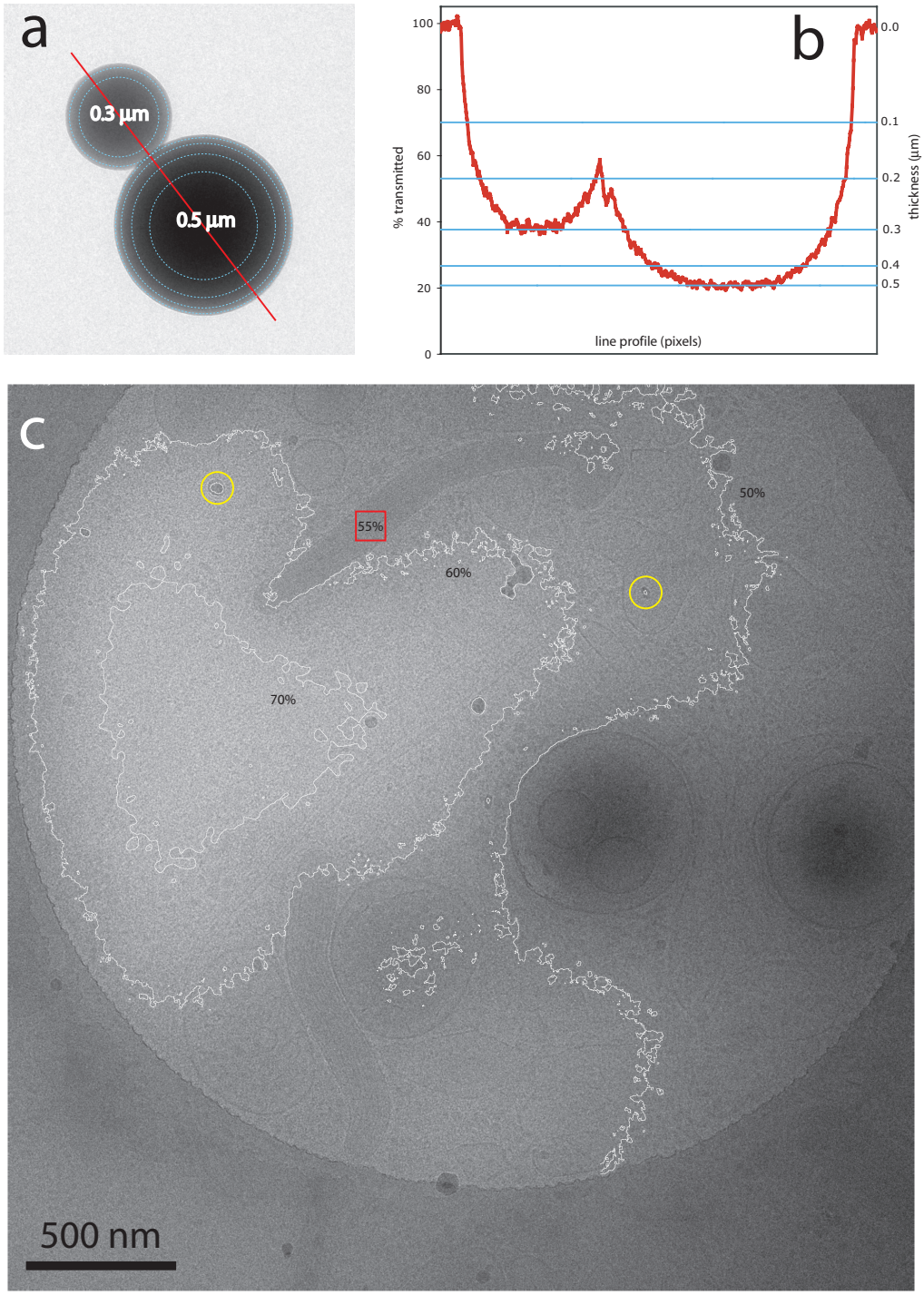

Fig. S1. Endothelial cell thickness is measured by electron scattering. Specimen thickness was estimated by measuring the percentage of the electron beam transmitted through the specimen to the camera, and calibrating the values against latex spheres (1) of density of 1.05 g/cc (Dow Chemicals), a value similar to that of cell cytoplasm calculated from its protein dry weight (2) and assuming 1.35 g/cc for the density of protein. This was performed online during a microscopy session to select suitable areas of the specimen. (*a*) Single low dose image of 0.3 μm and 0.5 μm latex spheres recorded using imaging parameters identical to those used for images of cells at 120 keV. Dotted lines indicate radii with calculated thicknesses of 0.1, 0.2, 0.3, and 0.4 μm, where the sphere center has a thickness equal to the sphere diameter. (*b*) Profile of intensity along the line drawn across both particle diameters in (*a*), given as percent transmission (*y* axis, left side) compared to background (100%) and as thickness (*y* axis, right side) corresponding to radii in (*a*). The resulting empirical curve deviates from the theoretical projection of a sphere at large values of thickness due to plural scattering (3). (*c*) Image of the cell corresponding to Fig. 2 and Movie S2. Contours correspond to 70% (0.1 μm), 60% (0.15 μm), and 50% (0.2 μm) transmission (thickness), where 100% transmission is recorded over an empty hole in the specimen under identical microscope conditions. Contours were calculated from the same image after low-pass filtering (ImageJ script courtesy of J.E.Molloy available). Percent transmission was converted to sample thickness according to the plot in (*b*). Circles indicate features located on the top and bottom of the specimen at a thickness less than 0.2 μm as determined from measurements on tomogram volumes or by stereometry in tilt series, thus corroborating estimates from latex spheres. WPBs scatter about 10% more than the adjacent cytoplasm, consistent with their identification in percoll gradient fractions at densities between 1.08 and 1.12 (4, 5) compared to 1.05 for cytoplasm.

1. Linders PW, Stols AL, Stadhouders AM (1983) Calibration of transmission electron microscopic mass determination using objects with known mass distribution. *J Microsc* 130:85–92.
2. Richter K (1994) High-density morphologies of ice in high-pressure frozen biological specimens. *Ultramicroscopy* 53:237–249.
3. Steven AC, Hainfeld JF, Wall JS, Steer CJ (1983) Mass distributions of coated vesicles isolated from liver and brain—Analysis by scanning-transmission electron microscopy. *J Cell Biol* 97:1714–1723.
4. Ewenstein BM, Warhol MJ, Handin RI, Pober JS (1987) Composition of the Von Willebrand-factor storage organelle (Weibel-Palade body) isolated from cultured human umbilical vein endothelial cells. *J Cell Biol* 104:1423–1433.
5. Vischer UM, Wagner DD (1993) CD63 Is a component of Weibel-Palade bodies of human endothelial cells. *Blood* 82:1184–1191.

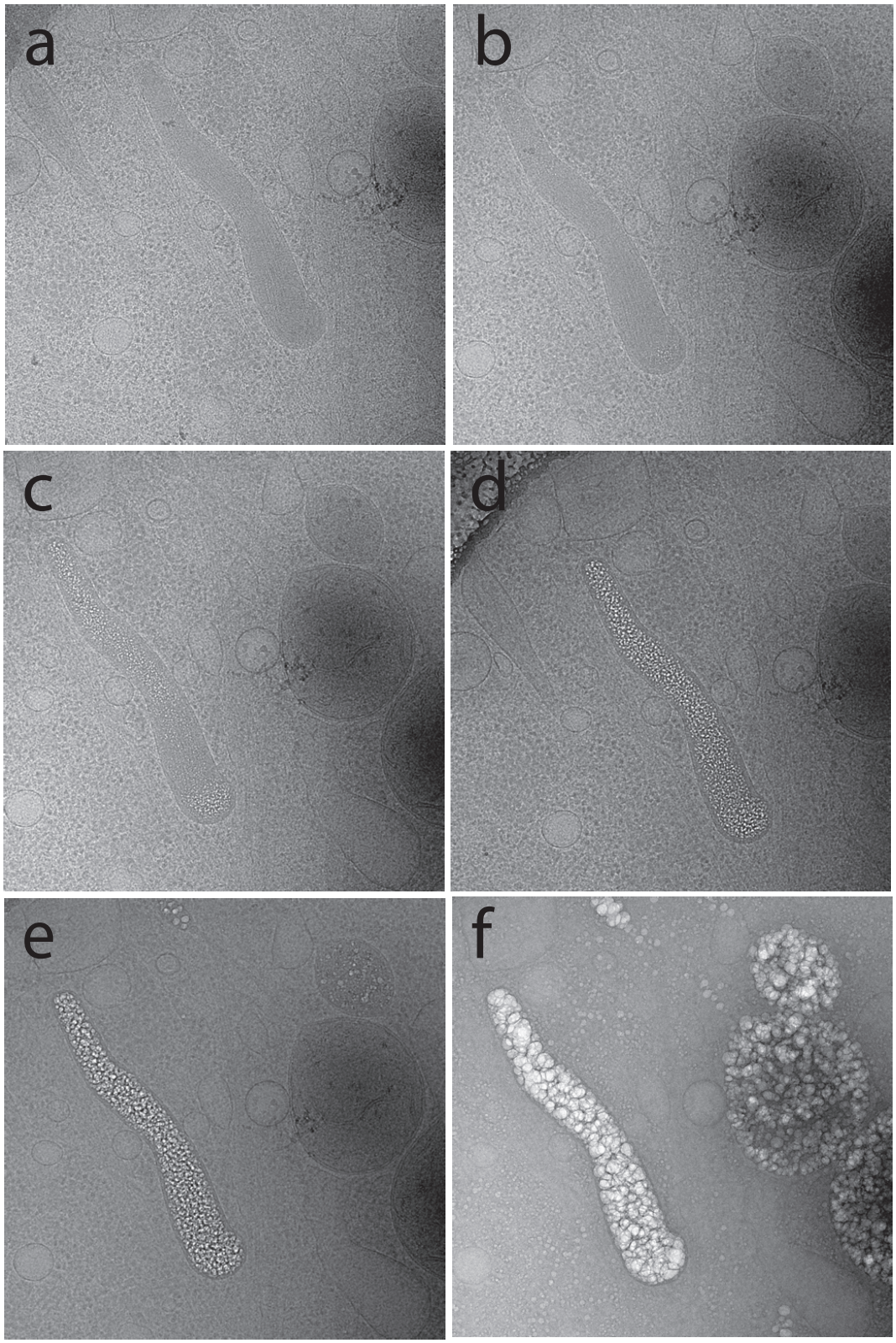

Fig. S2. Series of low dose images using 300 keV electrons of the cell periphery of a vitrified endothelial cell at liquid nitrogen temperature shows selective bubbling of the content of a WPB. Accumulated dose for frame (*a*) 70 $e^{-}/Å^2$, (*b*) 85 $e^{-}/Å^2$, (*c*) 100 $e^{-}/Å^2$, (*d*) 110 $e^{-}/Å^2$, (*e*) 140 $e^{-}/Å^2$, and (*f*) >250$e^{-}/Å^2$. Bubbling begins in frame (*b*) for the WPB, but not in the adjacent mitochondria. The small mitochondrion shows bubbling in frame (*e*). Frame (*f*) shows bubbling everywhere, including cytoplasm.

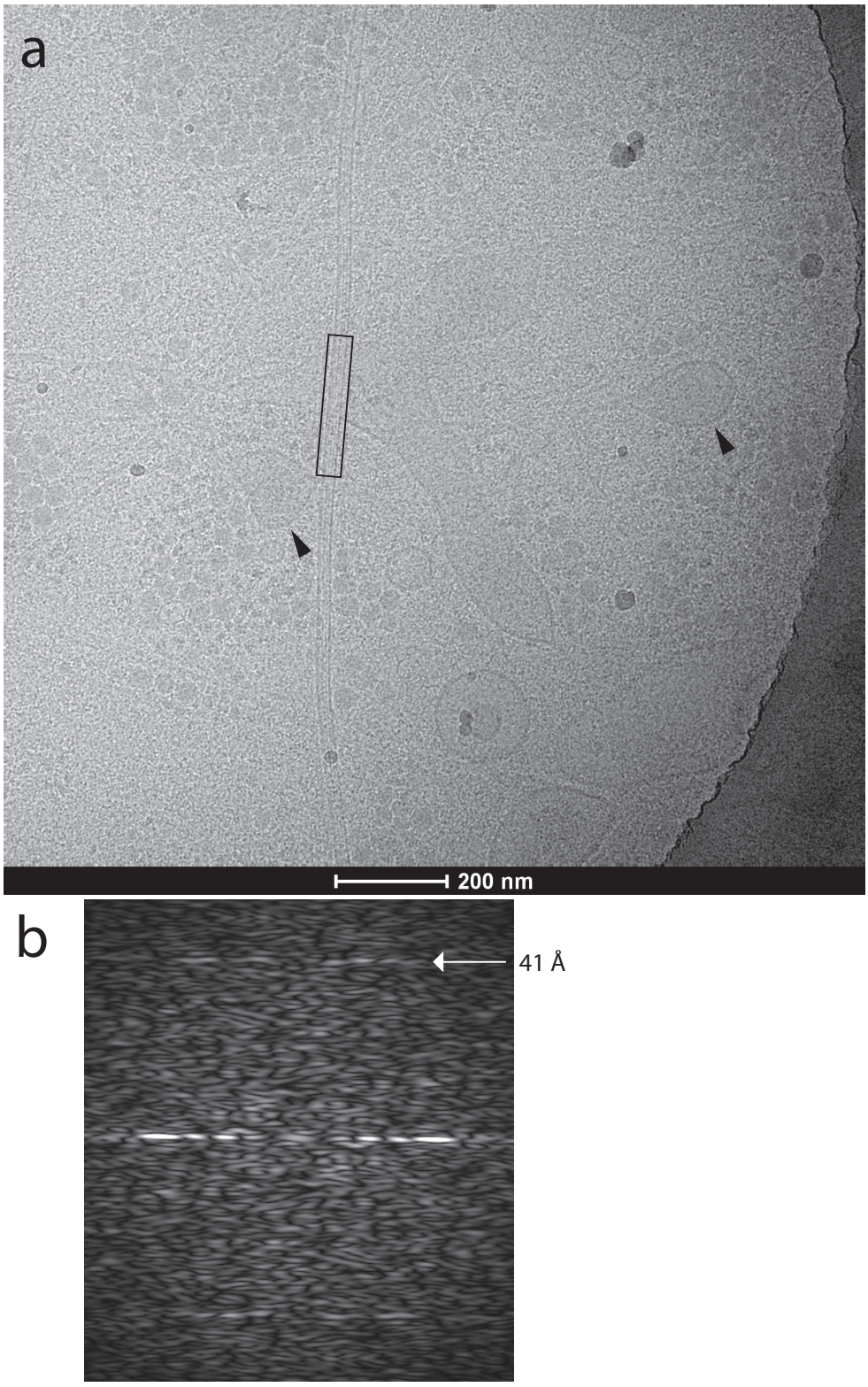

Fig. S3. Microtubules and ribosome-sized densities. (*a*) Microtubule and membranous organelles in a 0.1-μm thick region of a vitrified endothelial cell. A microtubule runs vertically in the image, a segment of which is boxed. A bi-lobed membrane structure is indicated by black arrows at each lobe and should be compared to similar structures in Fig. 2. (*b*) Fourier transform of the boxed area shows a layer line at 41 Å (arrow) typical for MTs and indicating a good preservation of structure. (*c*) Location of ribosome-sized densities identified in the electron tomogram in Movie S2 shown with a single slice of the tomogram. Also shown is the sum of projections of 380 ribosome-sized densities (left inset) and sum of 100 projections of the 80S ribosome map (right inset). See *SI Text*. (*d*) Low dose image at 120 keV of the same area of the specimen as shown in (*c*) with Body A, cytoskeletal filaments, and other cell content in projection.

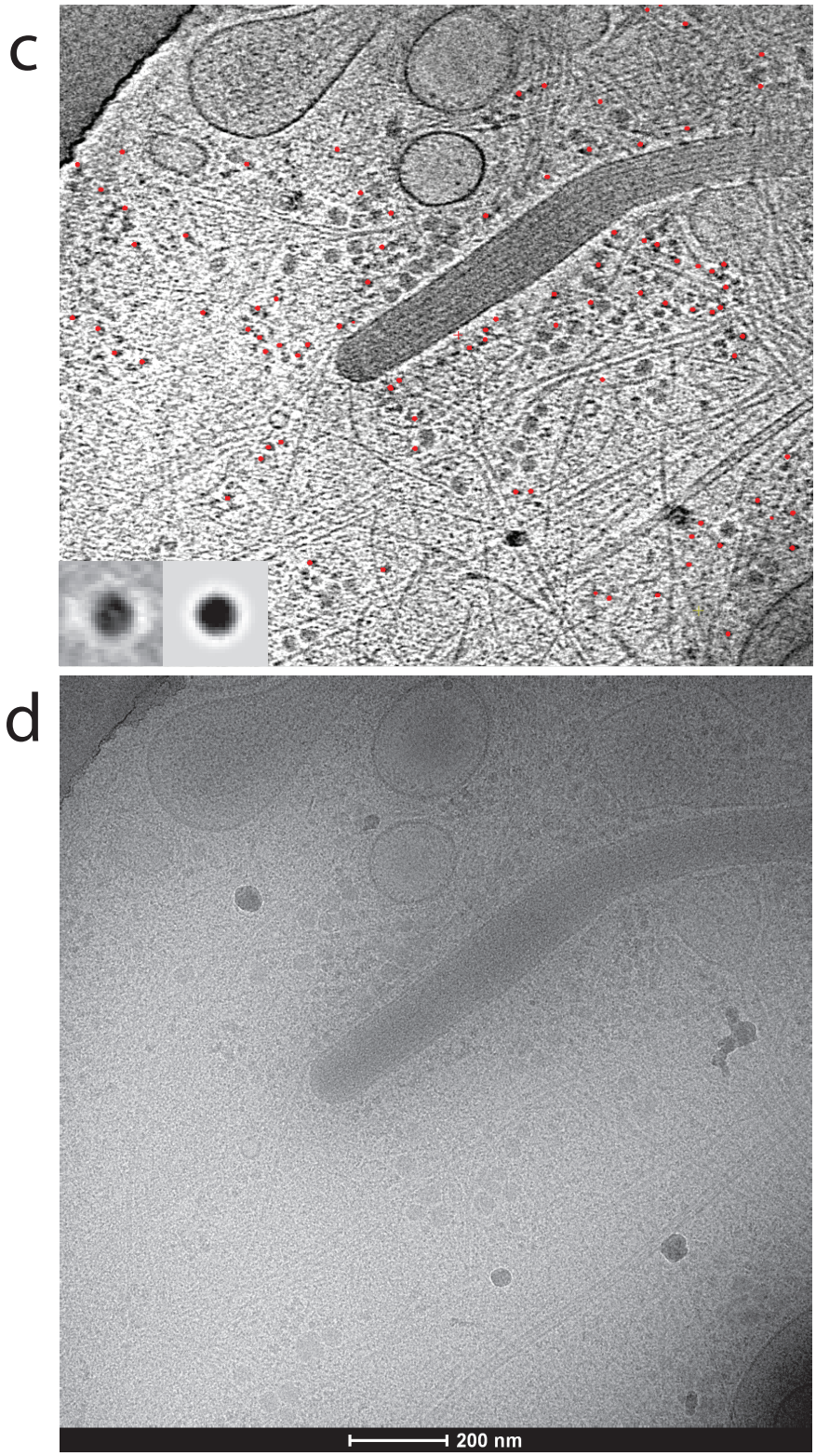

Fig. S3. Continued.

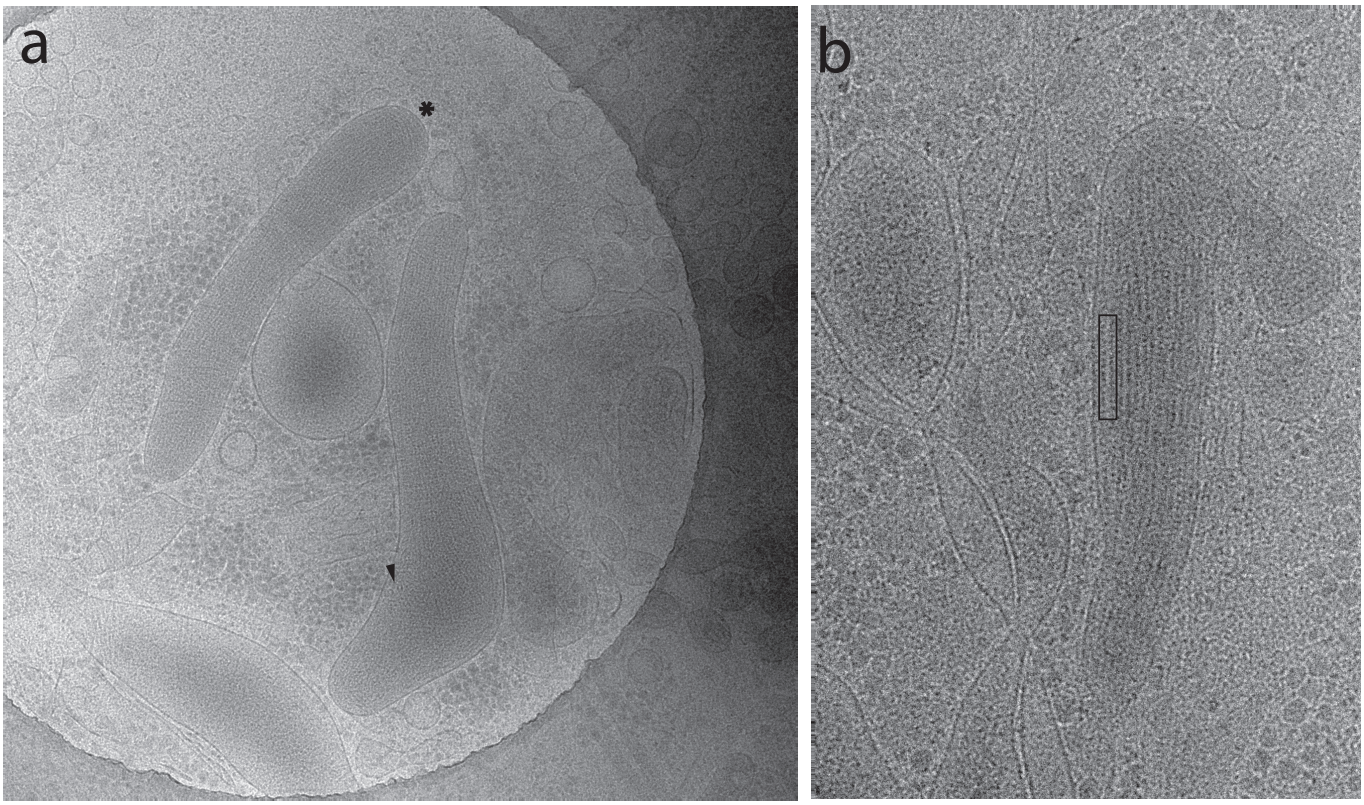

Fig. S4. WPBs of less regular shape. (*a*) Image recorded at 120 keV shows that VWF tubules curve at a rounded end (asterisk) and VWF tubules are poorly aligned where the body deviates from a rod-shaped structure near the black arrow which points at two VWF tubules seen end-on. (*b*) Image recorded at 300 keV with a black box around the tubule shown in Fig. 3*D*.

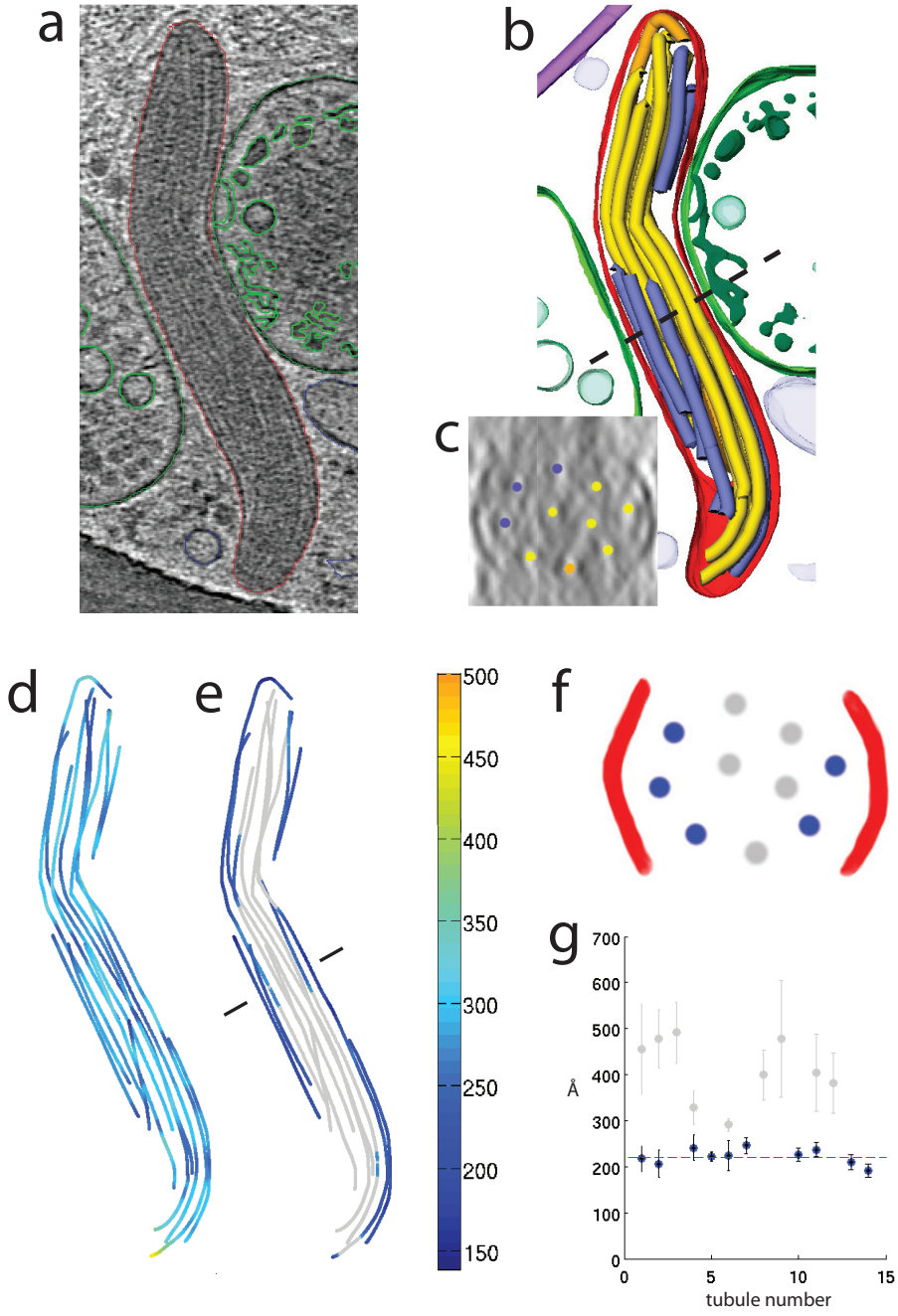

Fig. S5. Structural model for VWF tubules and the WPB membrane. (*a*) Section of a tomogram showing segmentation contours for membranes (WPB membrane is red, MVB membranes are green) drawn at the high contrast boundary between the outer edge of the membrane and the cytoplasm. (*b*) Model based on the segmentation shown in Movie S3. (*c*) 250 Å projected tomogram cross-section at the point indicated by dashed black line in (*b*) including tubule model positions. (*d*) Tubule model colored according to the inter-tubule distance (scale in Å at right), defined for each point as the minimum distance to a neighboring tubule. Average inter-tubule distance is 284 Å +/-31.3 Å. [pixel size = 27.6 Å] (*e*) Tubule model colored according to tubule-to-membrane distance *d* ($d < 280$ Å as per scale, but gray for $d > 280$ Å) highlighting those tubules that pack against the membrane in blue. (*f*) Cross-section through membrane and tubule model at position indicated and color as in (*e*). The membrane model (red) is incomplete due to the missing tomographic data wedge, but the tubule-to-membrane distance calculation is unaffected for tubules close to the membrane. (*g*) Distance between tubules and the membrane model (with standard deviations). Each of the 14 tubules (numbered on *x* axis) may have two tubule-to-membrane distance scores [*y* axis, points colored as in (f)] if a part follows the membrane but another part kinks away. Tubules that are close to the membrane model follow at a regular distance of 220 Å. The tubule-to-membrane distance (after subtracting the membrane thickness, 50–75 Å, which is included within the membrane model) is similar to half the distance between tubules, 140 Å, so that tubules are packed as closely to the membrane as they are to adjacent tubules.

Movie S1. EM tilt series recorded at the cell periphery using 120 keV electrons of a vitrified endothelial cell at liquid nitrogen temperature showing WPBs and other organelles including coated vesicles. Each frame is a low dose image of the specimen after rotation of the specimen stage from −50°(first frame) to + 35°(last frame) in 5° steps. [Note: images were acquired first from 0 to + 35° and then from −5° to −50°.] Several WPBs show a bubbling of internal contents due to radiation damage from accumulating electron dose (total dose $>50e^{-}/Å^{2}$).

Movie S1 (MOV)

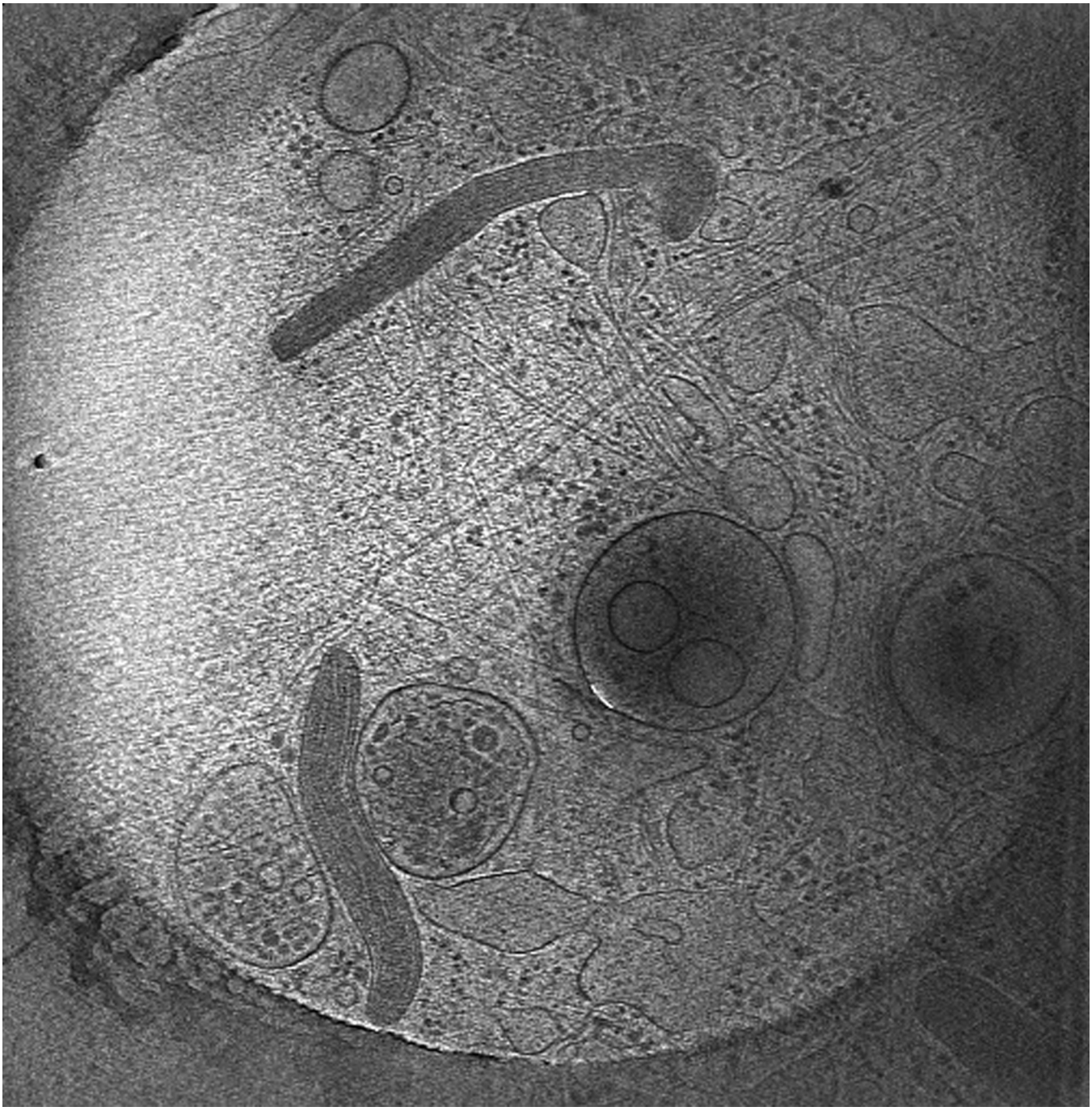

Movie S2. Electron tomogram of the endothelial cell periphery with two WPBs. Each frame is a slice through the tomogram. The field of view is annotated in Fig. 2.

Movie S2 (MOV)

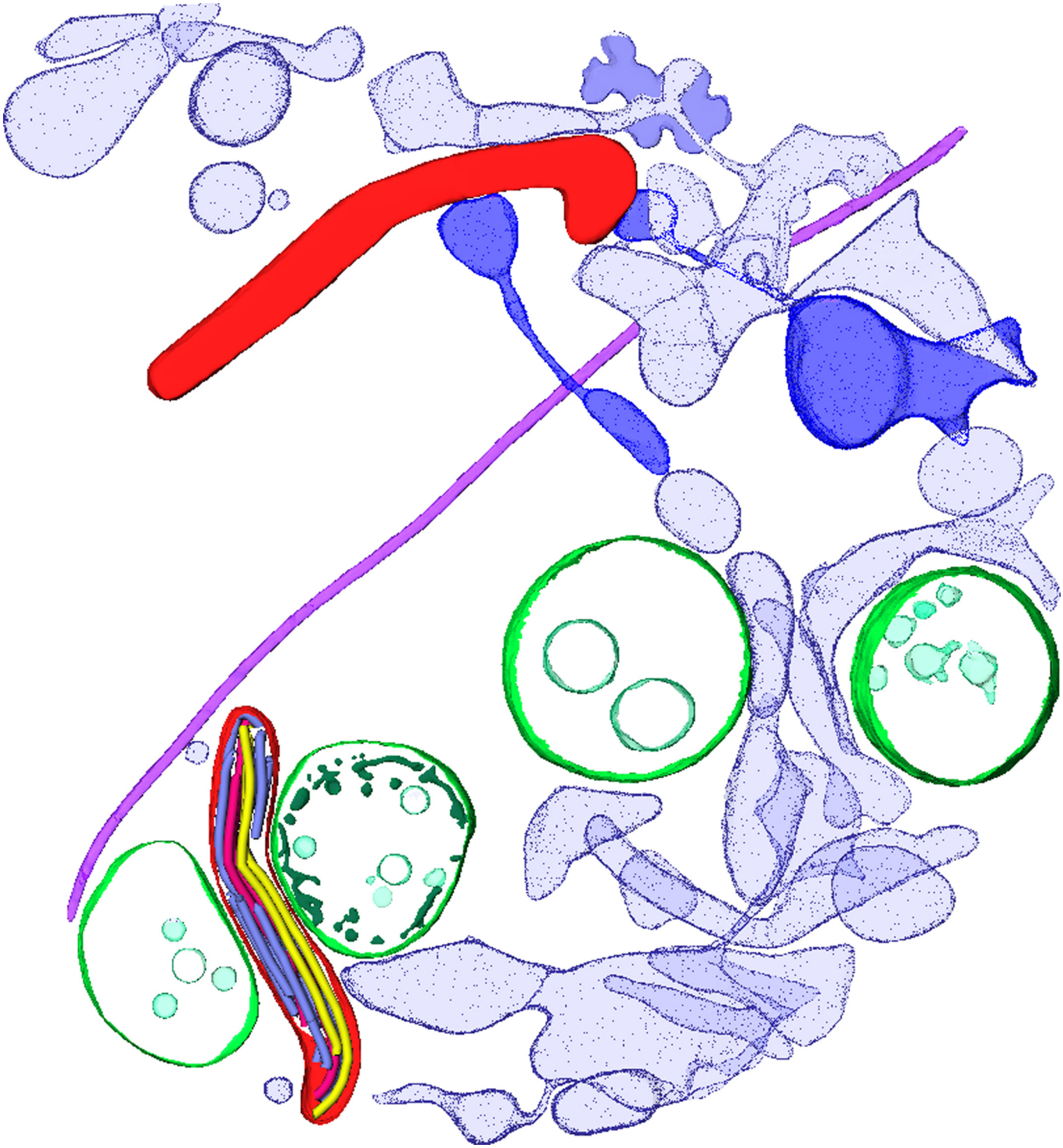

Movie S3. Segmentation of the electron tomogram in Movie S2 showing WPBs (red membranes), VWF tubules inside WPB membrane (yellow, blue, and red), multivesicular bodies/late endosome (green membranes), other membranes (blue), microtubule (purple).

Movie S3 (MOV)

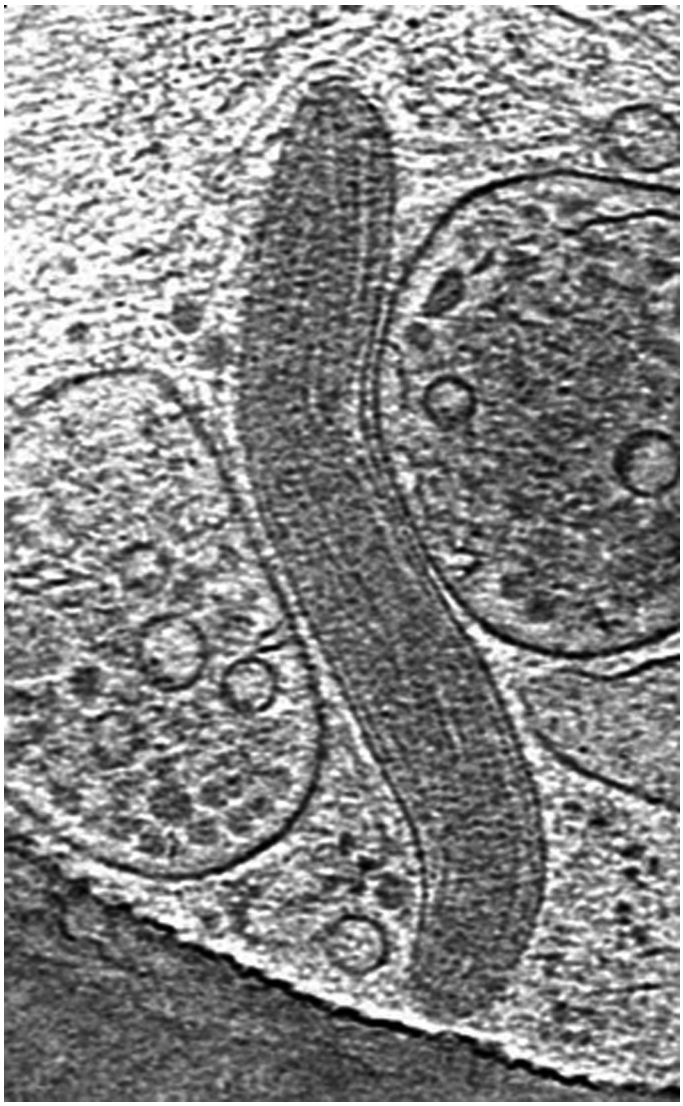

Movie S4. Electron tomogram of a WPB. Each frame is a slice through a tomogram which is a subvolume of the tomogram shown in Movie S2. The WPB is between two multivesicular bodies and is labeled body B in Fig. 2. Yellow lines show the trajectory of filaments in the model for the tubules.

Movie S4 (MOV)

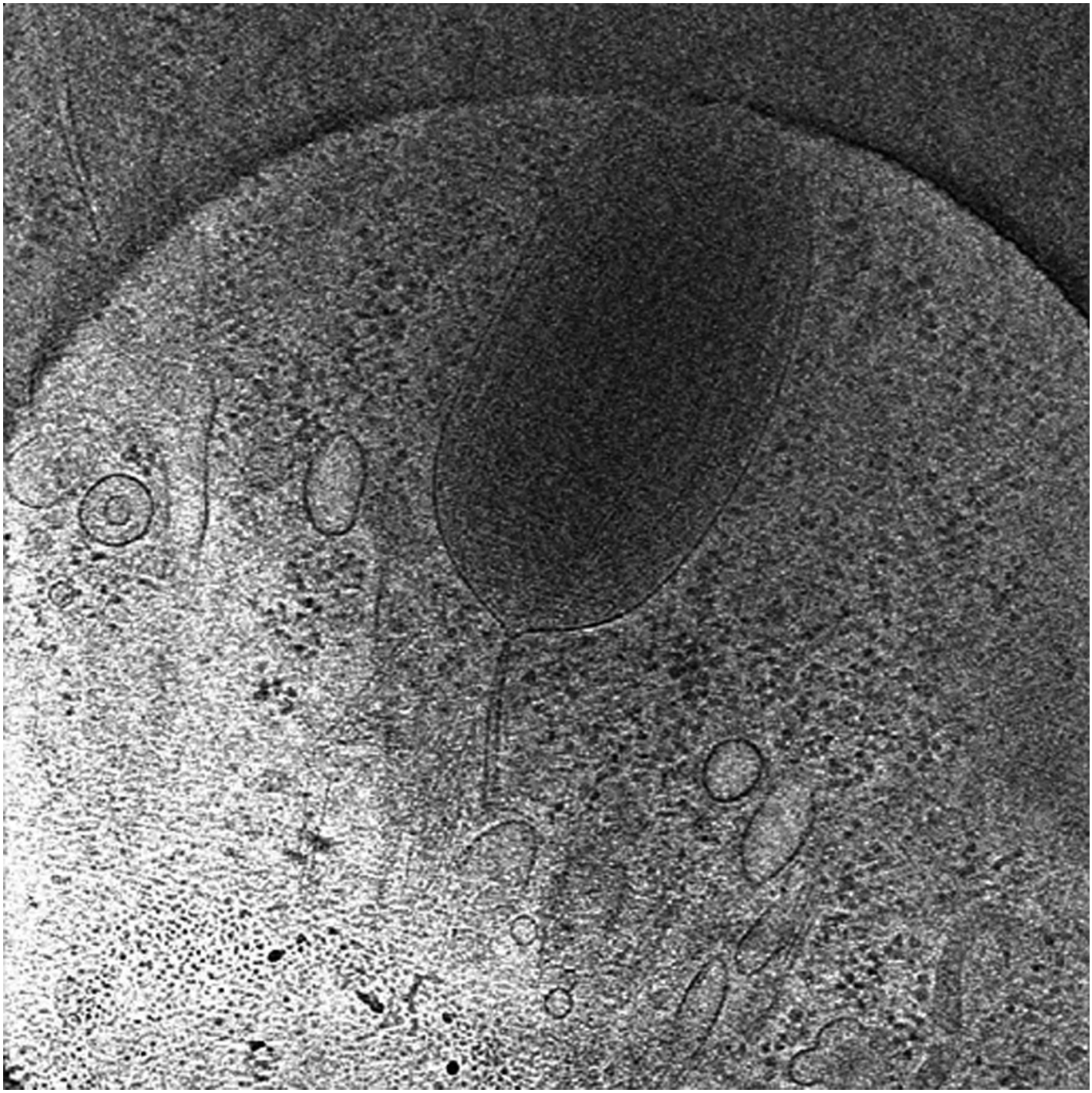

Movie S5. Electron tomogram of a marrow-shaped WPB. Each frame is a slice through the tomogram. A section of the tomogram is shown in Fig. 5*D*.

Movie S5 (MOV)

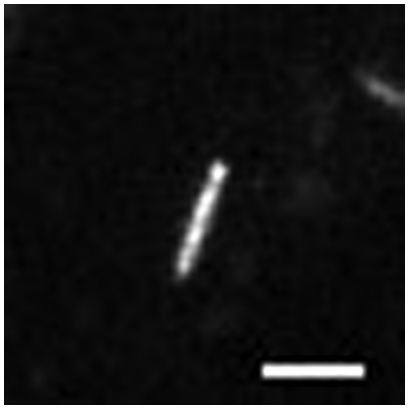

Movie S6. Live cell fluorescence image of WPB exocytosis. HUVECs expressing EGFP-CD63 were imaged at 7 frames/s during histamine stimulation. (Scale bar, 1 μm.) The image montage in Fig. 5*E* includes every second frame of the event.

Movie S6 (MOV)

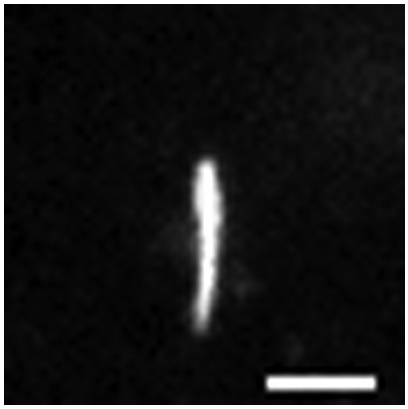

Movie S7. Live cell fluorescence image of WPB exocytosis. HUVECs expressing EGFP-CD63 were imaged at 7 frames/s during histamine stimulation. (Scale bar, 1 μm.)

Movie S7 (MOV)